Acta Neuropathol (2013) 125:861–878
DOI 10.1007/s00401-013-1111-z

ORIGINAL PAPER

Clathrin adaptor CALM/PICALM is associated with neurofibrillary tangles and is cleaved in Alzheimer's brains

Kunie Ando · Jean-Pierre Brion · Virginie Stygelbout · Valérie Suain · Michèle Authelet · Robert Dedecker · Anaïs Chanut · Pascale Lacor · Jérémie Lavaur · Véronique Sazdovitch · Ekaterina Rogaeva · Marie-Claude Potier · Charles Duyckaerts

Received: 20 October 2012 / Revised: 20 February 2013 / Accepted: 24 March 2013 / Published online: 16 April 2013

Abstract PICALM, a clathrin adaptor protein, plays important roles in clathrin-mediated endocytosis in all cell types. Recently, genome-wide association studies identified single nucleotide polymorphisms in *PICALM* gene as genetic risk factors for late-onset Alzheimer disease (LOAD). We analysed by western blotting with several anti-PICALM antibodies the pattern of expression of PICALM in human brain extracts. We found that PICALM was abnormally cleaved in AD samples and that the level of the uncleaved 65–75 kDa full-length PICALM species was significantly decreased in AD brains. Cleavage of human PICALM after activation of endogenous calpain or caspase was demonstrated in vitro. Immunohistochemistry revealed that PICALM was associated in situ with neurofibrillary tangles, co-localising with conformationally abnormal and hyperphosphorylated tau in LOAD, familial AD and Down syndrome cases. PHF-tau proteins co-immunoprecipitated with PICALM. PICALM was highly expressed in microglia in LOAD. These observations suggest that PICALM is associated with the development of AD tau pathology. PICALM cleavage could contribute to endocytic dysfunction in AD.

Keywords Alzheimer's disease · PICALM · Tau · NFT · Microglia

Electronic supplementary material The online version of this article (doi:10.1007/s00401-013-1111-z) contains supplementary material, which is available to authorized users.

K. Ando · A. Chanut · V. Sazdovitch · C. Duyckaerts
Laboratoire de Neuropathologie Escourolle,
Hôpital de la Pitié-Salpêtrière, AP-HP, Paris, France

K. Ando · J. Lavaur · M.-C. Potier · C. Duyckaerts (✉)
Group of Alzheimer's and Prion's diseases, ICM Research Centre, UPMC, INSERM UMR S 975, CNRS UMR 7225,
Hôpital de la Pitié-Salpêtrière, 47 Bd de l'Hôpital,
75013 Paris, France
e-mail: charles.duyckaerts@psl.aphp.fr

J.-P. Brion · V. Stygelbout · V. Suain · M. Authelet · R. Dedecker
Laboratory of Histology, Neuroanatomy and Neuropathology, UNI (ULB Neuroscience Institute), Université Libre de Bruxelles, 1070, Brussels, Belgium

P. Lacor
Neurobiology Department, Northwestern University, Evanston, IL 60208, USA

E. Rogaeva
Centre for Research in Neurodegenerative Diseases, Faculty of Medicine, University of Toronto, Toronto, Canada

Introduction

Alzheimer disease (AD) is characterised by two neuropathological hallmarks: amyloid plaques composed of extracellular aggregates of amyloid β (Aβ) peptide and neurofibrillary tangles (NFTs) made of intracellular aggregates of Paired Helical Filament (PHF)-tau proteins. While autosomal dominant, well characterised, mutations of the amyloid precursor protein (APP) and presenilin (PS1, PS2) genes have been identified in familial AD (FAD) cases, genetic risk factors for late-onset AD (LOAD) remained largely unknown until recently. Apolipoprotein E4 allele was, for a long time, the only well-characterised risk factor associated with LOAD. A dozen of new SNPs were recently identified in GWAS studies as risk factors [6, 29, 30, 41, 51, 61]. These polymorphisms involved genes coding for proteins that have roles in endocytosis, cholesterol metabolism or transport, and inflammation. *PICALM* (phosphatidylinositol-binding clathrin assembly protein), encoding a clathrin adaptor protein, was one of the genes most significantly

associated with LOAD risk in these studies. However, the role of PICALM in AD aetiology has yet to be understood.

PICALM/CALM was first cloned as a gene fused with AF10 in acute myeloid leukaemia model cell line U937 [23]. PICALM protein is involved in clathrin-mediated endocytosis occurring at the plasma membrane [65]. PICALM knock out mice exhibit severe growth retardation due to deficits in iron uptake [63]. Whereas PICALM is ubiquitously expressed, its homolog AP180 (also known as AP-3, NP185, pp155, Fl-20) is neuron specific [62, 76, 77]. Although AP180 and PICALM have similar functions such as controlling clathrin assembly and the size of clathrin-coated vesicles [1, 48, 50, 56, 79, 80], they do not co-localise in neurons [56, 77]. PICALM is composed of two major domains: AP180 N-terminal homolog (ANTH) domain at the N-terminus and clathrin-binding domain at the C-terminus. ANTH domain of PICALM contains both a membrane-associating sequence [24] and R-SNARE-binding region [24, 38, 49]. C-terminal unstructured domain of PICALM binds to AP-2 adaptor complex, clathrin heavy chain, epsin and synaptojanin [7].

PICALM ortholog, YAP1802, was identified as a modifier of Aβ toxicity in a genome-wide screen in yeast [68]. In addition, PICALM partially suppressed the toxicity of oligomeric Aβ in *C. elegans* and rat cortical neurons [68]. Although all these data point to a strong association of PICALM with AD aetiology, little is known on the levels of PICALM, its localisation and post-translational modifications in post-mortem human AD brains. Data from the literature are contradictory. Indeed, previous studies have reported that the expression level of *PICALM* mRNAs were either not significantly altered in AD prefrontal cortex [9] and in AD superior frontal gyrus [19, 78] or significantly increased in AD frontal cortex [4]. Using an anti-PICALM C-terminal antibody, PICALM immunoreactivity was either detected mainly in endothelial cells and only weakly in neuronal/glial cells in human brain sections [4], or very strongly detected in neurons but not in glial cells in mouse brain sections [74]. We have studied the distributions and expression levels of PICALM using three different PICALM antibodies in post-mortem brains from control, LOAD, FAD and Down syndrome patients. We have also used immunoprecipitation to analyse the relationship between tau and PICALM.

Materials and methods

Antibodies

The antibodies used in this study are listed in Table 1. Rabbit anti-PICALM antibodies (HPA019053, HPA019061) were purchased from SIGMA. Goat polyclonal anti-PICALM antibody C18 (sc-6433) was purchased from Santa Cruz biotechnology. The B19 antibody is a rabbit polyclonal antibody raised against adult bovine tau proteins, reacting with adult and foetal tau isoforms from bovine, rat, mouse and human nervous tissues in a phosphorylation-independent manner [13]. Mouse monoclonal anti-pSer202/Thr205 antibody AT8 was purchased from Pierce (MN1020). Mouse

Table 1 Primary antibodies

Antigen	Name	Antigen epitope	Dilution (IF, WB)	Host animal	Source
PICALM	HPA019053	Human PICALM 447–545	1/50, 1/2,000	Rabbit	SIGMA
PICALM	HPA019061	Human PICALM 263–343	1/10, 1/200	Rabbit	SIGMA
PICALM	sc-6433	Human PICALM 634–651	1/50, 1/50	Goat	SCBT
Tau	B19	Full length-bovine tau	1/50, 1/2,000	Rabbit	Dr. Brion
pTau	AT8	pSer202/pThr205	1/50, 1/2,000	Mouse	Pierce
Tau	Alz50	Tau in pathological conformation	1/50, –	Mouse	Dr. Davies
Tau	MC1	Tau in pathological conformation	1/50, –	Mouse	Dr. Davies
pTau	TG3	pThr231 + conformation	1/50, –	Mouse	Dr. Davies
pTau	PHF1	pSer396/404	1/50, –	Mouse	Dr. Davies
Tau-Asp421	36-017	Cleaved tau at Asp421	1/100, –	Mouse	Millipore
Aβ	6E10	Human Aβ 1–16	1/200, 1/2,000	Mouse	Covance
α-Synuclein	Hat3c	16 residues from C-terminus	1/100, –	Mouse	Dr. Clayton
CD68	M0814	Human macrophage	1/50, –	Mouse	Dako
GFAP	Ab10062	Human GFAP	1/50, –	Mouse	Abcam
Actin	8H10D10	N-terminus	–, 1/1,000	Mouse	Cell signaling
Cleaved caspase-3	5A1E	N-terminus adjacent to Asp175	–, 1/2,000	Rabbit	Cell signaling

PICALM numbering is according to PICALM isoform 1. Tau numbering is according to the longest 4R2N isoform

IF Immunofluorescence, *WB* western blotting

monoclonal anti-cleaved tau (Asp421) antibody, clone C3 (36-017) was purchased from Millipore. Mouse monoclonal anti-tau antibodies recognising tau pathological conformations (Alz50, MC1), pThr231 tau in pathological conformation form (TG3), and pSer396/404 tau (PHF1) were kindly provided by Dr. Peter Davies (Albert Einstein College of Medicine, NY). Mouse monoclonal anti-GFAP antibody (ab10062) was purchased from Abcam. Mouse monoclonal anti-CD68 antibody (M0814) was purchased from Dako. Mouse monoclonal anti-Aβ antibody 6E10 was purchased from Covance. Mouse monoclonal anti-α synuclein antibody Hat3c was a kind gift from Drs George and Clayton (University of Illinois, USA) [26]. Mouse monoclonal anti-β actin antibody (8H10D10, #3700) and rabbit monoclonal anti-cleaved caspase-3 antibody (5A1E, #9664) were purchased from Cell Signaling.

Brain tissues

Control non-demented and AD individuals were enrolled in a brain donation programme of the national network of Brain Bank, GIE NeuroCEB, organised by a consortium of Patients Associations. An explicit consent had been signed by the patient or by the next of kin, in the name of the patient. The project was approved by the scientific committee of the Brain Bank. The whole procedure of the Brain Bank has been reviewed and accepted by the Ethical Committee "Comité de Protection des Personnes Paris Ile de France VI" and has been declared to the Ministry of Research and Higher Education as requested by the French law.

Samples from the hippocampus and temporal isocortex were obtained from individuals with LOAD, FAD and Down syndrome, P301L *MAPT* mutation and LBD as well as from controls as listed in Table 2. Substantia nigra from the LBD case was also studied. AD cases were diagnosed according to the National Institute of Aging and Reagan Institute Criteria [5]. AD cases and the Down syndrome case were all scored Braak's stages V or VI. FAD cases were associated with APP or PS1 mutations (Table 2). Control cases were non-demented individuals who died without known neurological disorders. The mean age at death and post-mortem delays of control cases and of AD patients (Table 1) were not significantly different. Average age at death was 67.92 ± 2.8 and 70.38 ± 3.7 years for control and AD cases (including FAD cases), respectively (mean ± SEM). Average post-mortem delays were 23.86 ± 3.6 and 23.95 ± 4.3 h for control and AD cases (mean ± SEM).

Table 2 Human cases analysed in this study

Case#	Clinical diagnosis	Braak stage	Thal stage plaque score	PMD (h)	Age (years)	Sex	Analysis
1	Control	II	0	10	73	M	WB
2	Control	0	1	13.5	84	M	WB
3	Control	0	0	7	66	M	WB
4	Control	II	0	NA	79	M	WB
5	Control	0	0	20	61	M	IHC
6	Control	0	0	32	67	M	IHC
7	Control	III	0	30	70	M	IHC
8	Control	II	0	26	66	M	IHC
9	Control	I–III	0	49	74	F	IHC
10	Control	0	0	NA	58	F	IHC
11	Control	0	0	17	46	F	IHC
12	Control	IV	1	29	77	F	IHC
13	Control	0	0	29	62	F	IHC
14	AD	VI	5	22	70	M	WB
15	AD	VI	5	9.5	66	M	WB
16	AD	VI	5	10	74	M	WB
17	AD	VI	5	6	71	M	WB
18	AD	VI	5	45	73	M	IHC
19	AD	VI	4	34	83	M	IHC
20	AD	VI	4	24	80	F	IHC
21	AD	V	5	50	87	F	IHC
22	AD	VI	5	24	83	F	IHC
23	AD	VI	4	24	79	F	IHC
24	FAD (APP G2149A)	VI	3	NA	56	F	WB
25	FAD (PS1 M233T)	VI	5	NA	43	F	IHC
26	FAD (PS1 R35E, E120D)	VI	5	15	50	F	IHC
27	Down syndrome	VI	5	NA	58	M	IHC
28	P301L *MAPT*	0	0	30	66	M	IHC
29	LBD	II	0	48	63	M	IHC

The neuropathological staging of AD patients is determined according to Braak and Braak [11] and to Thal et al. [66] for amyloid plaque scores

Frozen tissues of isocortex were analysed by western blotting (WB). Paraffin-embedded tissues of hippocampus and isocortex were analysed by immunohistochemistry (IHC)

AD Alzheimer disease, *FAD* familial Alzheimer disease, *PMD* post-mortem delay, *NA* not available, *P301L MAPT* P301L microtubule associated protein tau mutation, *LBD* Lewy body disease, diffuse type

Preparation of brain homogenates for biochemical analysis

About 200 mg of frozen temporal isocortex was homogenised as reported [3] in 10 volumes of ice-cold RIPA buffer containing protease and phosphatase inhibitors (Tris 50 mM pH 7.4 containing 150 mM NaCl, 1 % NP40, 0.25 % sodium deoxycholate, 5 mM EDTA, 1 mM EGTA, Roche complete protease inhibitors, 1 mM PMSF, 25 μg/

ml Pepstatin, 50 mM β-Glycerophosphate, 10 mM sodium pyrophosphate, 10 mM sodium fluoride, 10 mM sodium orthovanadate) and incubated for 30 min at 4 °C on a rotator. One part of the homogenate was supplemented with Laemmli buffer, sonicated on ice and analysed as the total fraction. The rest of the homogenate was centrifuged (16,000×*g* for 20 min at 4 °C) and the supernatant was used as a RIPA-soluble fraction. The RIPA-insoluble pellet was re-suspended by sonication in fivefold volume of 8 M urea containing protease and phosphatase inhibitors and incubated for 30 min at room temperature on a rotator. The mixture was centrifuged at 16,000×*g* at 4 °C for 30 min. The supernatant was used as RIPA-insoluble fraction.

Sarkosyl fractionation was carried out as previously described [3, 14, 28]. To 1 ml of RIPA-soluble fraction of brain lysates at a protein concentration of 2 mg/ml, 10 mg of *N*-lauroylsarcosine sodium salt (L-5125; Sigma-Aldrich) was added to reach a final concentration of 1 % (w/v). The lysates were then incubated at room temperature for 30 min with a mild agitation followed by an ultracentrifugation at 180,000×*g* for 30 min at 4 °C. The sarkosyl-soluble supernatant was removed, and sarkosyl-insoluble pellets were rinsed briefly with 500 µl of 50 mM Tris–HCl (pH 7.4) and re-suspended in 200 µl of 50 mM Tris–HCl by vigorous pipetting. Sarkosyl-insoluble fractions were analysed by western blotting and transmission electron microscopy.

ADDLs (amyloid-beta-derived diffusible ligands) were prepared from biotinylated $A\beta_{1-42}$ peptide as previously described [40]. 10 µg/lane of ADDLs was applied to SDS-PAGE and analysed by western blotting.

Ultrastructural immunolabelling of PHF

Tissue blocks of the temporal isocortex of AD cases were fixed in glutaraldehyde 0.5 % (v/v), paraformaldehyde 4 % (v/v) in 0.1 M phosphate buffer, pH 7.4, and embedded in LR white resin. Ultrathin sections from LR white blocks were analysed by immunogold staining as previously described [15] using the anti-PICALM HPA019053 or PHF1 antibody. Grids with ultrathin sections were incubated overnight with the primary antibody, washed and then incubated for 2 h with anti-rabbit secondary antibodies conjugated to 15 nm colloidal gold or anti-mouse secondary antibodies conjugated to 10 nm colloidal gold particles (BBInternational, UK). Isolated PHFs present in sarkosyl-insoluble fraction were adsorbed on formvar-coated grids for transmission electron microscopy and also analysed by immunogold staining followed by negative staining with 1 % (w/v) sodium/potassium phosphotungstate, as previously described [12–14]. Ultrathin sections and formvar-coated grids were observed with a Zeiss EM 809 transmission electron microscope at 80 kV.

Cell culture

The human neuroblastoma cell line SKNSH-SY5Y (SY5Y) was cultured in Dulbecco's modified Eagle medium supplemented with 10 % foetal bovine serum and penicillin/streptomycin (Invitrogen) in a 5 % CO_2 humidified incubator at 37 °C. Cell lysates were prepared as previously described [22].

Calpain and caspase cleavage assays

In vitro cleavage of PICALM by calpain was analysed as previously described [58] in lysates of SY5Y neuroblastoma cells. The cells were harvested in HEPES buffer (20 mM HEPES, pH 7.4, 1 % Triton X-100, 100 mM KCl, 0.1 mM dithiothreitol, complete protease inhibitor tablet). Calpain cleavage was tested in the three following conditions: Condition 1—calpain was activated by adding 2 mM $CaCl_2$ to the lysate; Condition 2—the activation was inhibited by calcium chelators (2 mM EDTA + 2 mM EGTA were added to the lysates); Condition 3—calpain activation was blocked by pharmacological inhibitors (2 mM CaCl2 were added with 400 mM calpain inhibitors A6185 and A6060 from SIGMA). Aliquots of cell lysates were kept on ice for 30 min and were vortexed every 10 min for solubilisation. The lysate was then centrifuged at 20,000×*g* for 15 min. The supernatant was incubated at 22 °C for 1 h. The reaction was stopped by adding Laemmli buffer followed by incubation at 100 °C for 10 min and samples were analysed by western blotting.

Cleavage of PICALM by caspase-3 was studied in SY5Y neuroblastoma cells. SY5Y cells were incubated with 100 nM staurosporine (S4400, SIGMA) for 24 h to induce apoptosis [57] and compared to control cells incubated with only DMSO. Cells were collected in RIPA buffer, kept on ice for 30 min and aliquots were vortexed every 10 min, followed by centrifugation at 20,000×*g* for 15 min at 4 °C. The supernatant was mixed with Laemmli buffer and analysed by western blotting.

Western blot

Protein concentrations were estimated by the Bradford method (Bio-Rad). Tissue samples (20 µg/lane) were run in 10 or 12 % of Tris–glycine gels depending on the molecular weight of the protein of interest and transferred onto PVDF membranes (#162-0177, Bio-Rad). The PVDF membranes were blocked in 10 % (w/v) semi-fat dry milk in TBS (Tris 0.01 M, NaCl 0.15 M, pH 7.4) for 1 h at room temperature and were incubated with primary antibodies overnight followed by incubation with anti-rabbit (G-21234, Invitrogen), anti-mouse (G-21040, Invitrogen) or anti-goat (R-21459, Invitrogen) immunoglobulin conjugated to horseradish

peroxidase. Finally, membranes were incubated with SuperSignal West Pico Substrate (Pierce) and were exposed to an X-ray film (Pierce). Levels of proteins were estimated by densitometry analysis using the NIH Image J program. Anti-actin immunoblot was used to normalise protein loading.

Immunoprecipitation

The RIPA-soluble fraction of LOAD isocortex was pre-cleared for 1 h at 4 °C with Protein G Sepharose (P3296, SIGMA) and centrifuged at 14,000 rpm. The supernatants were then incubated with Protein G Sepharose and with or without 1.25 µg of the anti-PICALM HPA019053 antibody at 4 °C on a rotator overnight. The protein G beads were pelleted and washed three times with RIPA buffer. After the third wash, SDS sample buffer containing 5 % β-mercaptoethanol was added to the beads. Samples were heated at 100 °C and PICALM immunoprecipitates were analysed by western blotting for the presence of hyperphosphorylated tau and Aβ.

Histological staining and immunohistochemistry

After formaldehyde fixation (10 % buffered formalin), samples were paraffin embedded. Four micrometre-thick tissue sections of temporal isocortex and hippocampus were obtained. For immunolabelling with the PICALM antibodies, deparaffinised and rehydrated tissue sections were heated in citrate buffer for 20 min before incubation with the blocking solution. They were incubated in H_2O_2 to inhibit endogenous peroxidase, rinsed in water and then incubated with a blocking solution containing 2 % bovine serum albumin in TBS. Sections were then incubated overnight with the primary antibody. The presence of the primary antibody was visualised with the Dako REAL detection system (which includes both anti-rabbit and anti-mouse secondary antibodies) using diaminobenzidine (DAB) as chromogen. Biotinylated rabbit anti-goat IgG antibody (6164-08 Southern Biotech) was used for sc-6433 detection. Double immunofluorescent labelling was performed as previously reported [3], using goat anti-mouse antibody conjugated to Alexa 568 (A-11031, Invitrogen) and goat anti-rabbit antibody conjugated with Alexa 488 (A-11034, Invitrogen). Thiazin red staining was performed as previously described [47, 70]. Immunofluorescent labelling was observed with an upright confocal microscope (Olympus Fluoview Fv1000) or with an Axiovert 200M microscope (Zeiss) equipped with an ApoTome system (Zeiss).

To check for the specificity of the labelling, diluted anti-PICALM antibodies (Table 1) were pre-incubated with 15 µg/ml of GST-PICALM (157H00008301, tebu-bio) on a rotator at 4 °C overnight prior to immunohistochemistry.

Evaluation of PICALM-positive neurons and microglial cells

Sections immunostained for PICALM with DAB as chromogen were examined blind to diagnosis with a light microscope using a 10× objective, then examined in detail at higher magnifications. The intensity of PICALM immunoreactivity in PICALM-positive neurons and the numerical density of PICALM-positive microglial cells in hippocampus were scored subjectively by two observers on a scale of 0–3. The scoring took into account the whole section.

Statistical analysis

Statistical significance of comparisons between patients and controls was determined by unpaired Student's *t* test or by one-way ANOVA (with Bonferroni correction) using Prism 4 software (Graphpad).

Results

Specificity and titre of the anti-PICALM antibodies used in this study

In this study, we used three anti-PICALM polyclonal antibodies that recognise distinct epitopes (Table 1; Fig. 1a). The specificity of these anti-PICALM antibodies was first analysed by western blotting using lysates of SY5Y neuroblastoma cells (Fig. 1b). As expected, several bands around 65–75 kDa were detected with the three anti-PICALM antibodies corresponding to different PICALM isoforms generated by alternative splicing [4, 33, 67]. Several dilutions for each antibody were tested, and the optimal concentrations for western blotting were 1.4 µg/ml for HPA019061, 0.23 µg/ml for HPA019053 and 2 µg/ml for sc-6433 (antibody dilutions are shown in Table 1). The rabbit polyclonal anti-PICALM antibody HPA019053 was found to have the highest antibody titre (as shown by western blotting) and was preferentially used in this study.

PICALM was abnormally cleaved and its level was decreased in AD brains

In order to compare the level of expression of PICALM in control ($n = 4$) and AD brains (LOAD, $n = 4$; FAD with APP mutation, $n = 1$) (Table 2), frozen brain tissue samples from isocortex were homogenised in a modified RIPA buffer [3]. In the total fractions, the main PICALM

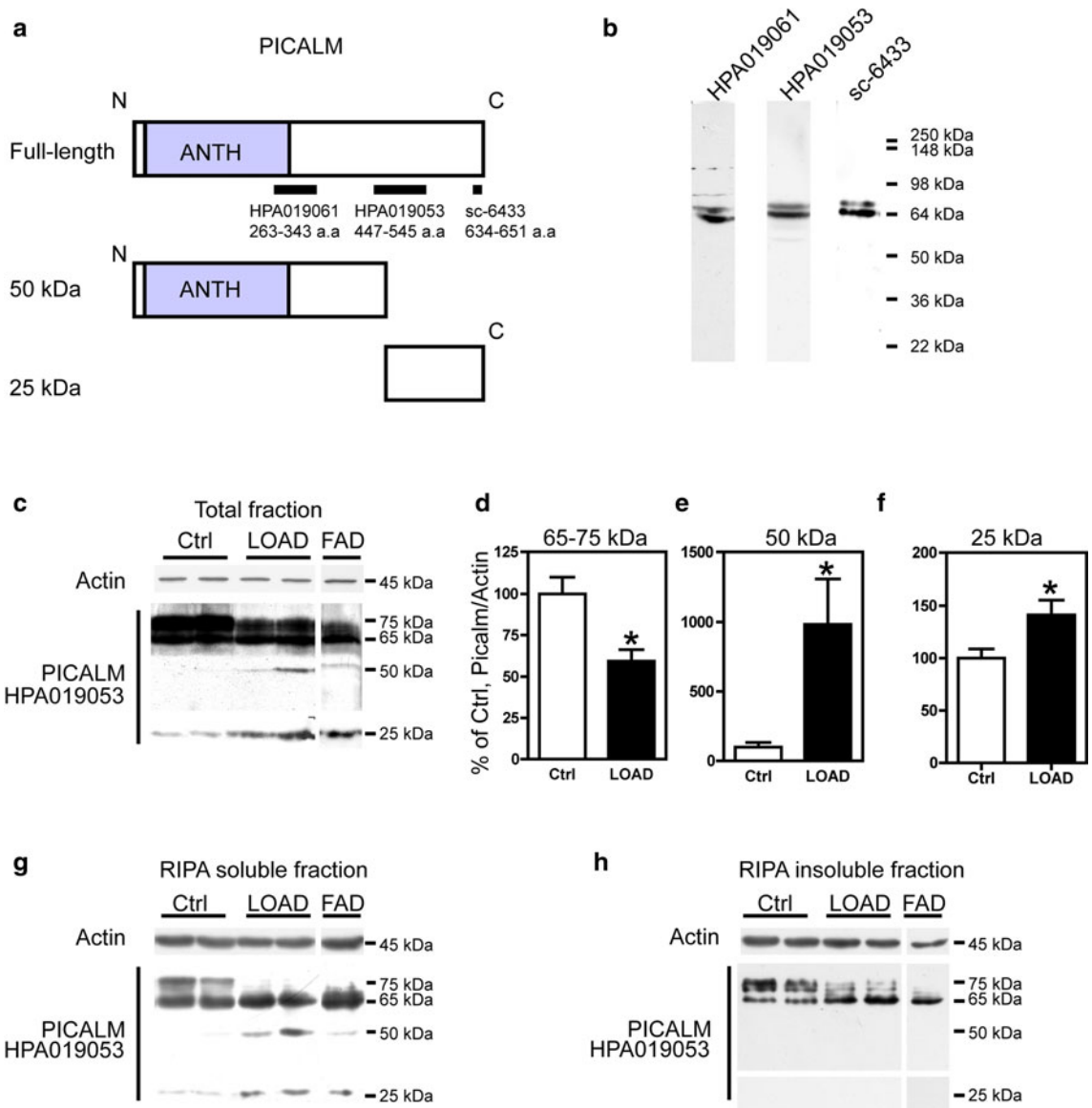

Fig. 1 Level of PICALM at 65–75 kDa was reduced and PICALM was abnormally cleaved in AD brain. **a** Schematic representation of PICALM full-length protein (isoform 1, 652 a.a.), localisation of the epitopes for the three anti-PICALM antibodies used in this study and putative cleaved fragments. **b** Western blot analysis of SH-SY5Y neuroblastoma cell lysates for PICALM. Cell lysates were subjected to SDS-PAGE followed by western blotting using different anti-PICALM antibodies as indicated. **c**–**h** Extracts of human non-demented control, LOAD and FAD brains were analysed by western blotting using anti-PICALM HPA019053 antibody for total (**c**), RIPA-soluble (**g**) and RIPA-insoluble (**h**) fractions. **d**–**f** Quantifications of the level of 65–75, 50 and 25 kDa PICALM species in total fraction normalised to actin. Full-length 65–75 kDa PICALM isoforms were reduced (**d**) and cleaved 50 kDa (**e**) and 25 kDa (**f**) PICALM fragments were increased in both LOAD and FAD brains. 4 control and 4 LOAD cases were analysed for statistical evaluation. $*p < 0.05$, by Student t test

immunoreactive bands identified with the anti-PICALM HPA019053 antibody corresponded to several isoforms of 65–75 kDa (Fig. 1c). Levels of full-length PICALM (65–75 kDa) showed more than 30 % decrease in AD brains as compared to controls (Ctrl, 100 ± 10.0; LOAD, 59.3 ± 6.7, mean ± SEM, $p < 0.02$) (Fig. 1c), most pronounced for the 75 kDa PICALM species. Two lower molecular weight species of 50 and 25 kDa (Fig. 1c), likely corresponding to cleaved forms of PICALM, were also identified. Levels of cleaved forms of PICALM were significantly increased in LOAD brains compared to non-demented controls (Ctrl, 100 ± 8.7; LOAD, 141 ± 13.8, $p < 0.05$ for 25 kDa; Ctrl, 100 ± 31.9; LOAD, 983 ± 327.0, $p < 0.05$ for 50 kDa; values are mean ± SEM) (Fig. 1e, f). In the FAD case with APP mutation, normalised PICALM 65–75 kDa bands were 75 % and cleaved fragments were 132 % for 25 kDa and 428 % for 50 kDa compared to the means of controls. The FAD data were in

the 95 % range of LOAD data and the western blot profile of PICALM in FAD case was not clearly distinguishable from the LOAD cases (Fig. 1c). These observations were confirmed in RIPA-soluble fractions, in which the level of the longest 75 kDa PICALM species was decreased and the levels of the cleaved 25 and 50 kDa forms increased in LOAD and FAD brains (Fig. 1g). Cleaved PICALM fragments were not detected in the RIPA-insoluble fraction, but the 75 kDa PICALM species was also decreased in this fraction (Fig. 1h). These data suggested that PICALM was abnormally cleaved in the brains of both LOAD and FAD and that the cleaved fragments were RIPA-soluble. Decrease of the 75 kDa PICALM species in RIPA-soluble fraction of AD brain was confirmed using the two other anti-PICALM antibodies (Fig. S1ab). The 50 kDa cleaved fragments could be detected with HPA019061 antibody (Fig. S1a), but not with the anti-PICALM C-terminal sc-6433 antibody (Fig. S1b). On the contrary, the 25 kDa cleaved fragment was detected with sc-6433 but not with HPA019061. This suggests that the 50 kDa fragment contains all or part of the PICALM amino domain and that the 25 kDa fragment contains the PICALM C-terminus and part of its carboxyl domain (Fig. 1a). To exclude the possibility that these PICALM-positive bands in AD brain could be due to cross-reactivity with Aβ oligomers, we studied by western blotting the reactivity of the anti-PICALM antibodies with ADDLs. None of the anti-PICALM antibodies used in this study showed unspecific cross-reactivity to oligomeric Aβ (Fig. S1c).

PICALM immunoreactivity was present in neurons, glial cells, and endothelial cells in control brains

A weak immunoreactivity was observed in the cell body of neurons with anti-PICALM HPA019053 antibody. A thin perinuclear rim was immunoreactive in neurons (Figs. 2a, 3a). Endothelial cells and epithelial lining of the choroid plexus were strongly labelled (Fig. S2a, d). Similar labellings were obtained with the anti-PICALM C-18 sc-6433 (Fig. S2c, f), but the immunostaining was of lower sensitivity, and unspecific labelling of lipofuscin was prominent. (Fig. S2i).

PICALM was highly expressed in neurons and microglia in LOAD brains

PICALM labelling of endothelial cells, ependymocytes and epithelial lining of the choroid plexus was similar in AD and control samples (Fig. S2). PICALM was more highly expressed in a few neurons, sometimes devoid of NFTs, in AD brains than in control cases (Fig. 2a–d). The intensity of the immunostaining of PICALM was significantly increased in the neurons of LOAD and FAD with PS1 mutations (ANOVA; $p < 0.05$). PICALM immunoreactivity was blindly and semi-quantitatively evaluated for neurons (Fig. 2d) and microglial cells (Fig. 2h). We noticed a significant increased density of PICALM-positive microglial cells in the hippocampus and temporal cortex of LOAD cases (but not in the FAD cases with PS1 mutations) compared to control cases (Fig. 2e–h)—semi-quantitative assessment; ANOVA; $p < 0.05$. Double staining for PICALM and glial markers confirmed that PICALM was highly expressed in CD68-positive activated microglial cells (macrophages) (Fig. 2i–k), but only weakly in GFAP-positive astrocytes (Fig. 2l–n) in LOAD. Oligodendrocytes were not PICALM positive (data not shown).

Association of PICALM immunoreactivity with neurofibrillary pathology in LOAD, FAD and Down syndrome

In samples from AD and Down syndrome patients, PICALM immunoreactivity was detected in neuronal inclusions with characteristic NFT shapes located in the cell bodies of some neurons (Fig. 3b–g), in dystrophic neurites associated with the amyloid plaques (Fig. 3g, black arrowhead), in neuropil threads and in granules of granulovacuolar degeneration (GVD) (Fig. 3d). PICALM-positive NFTs were more numerous in Down syndrome, lower in FAD and the lowest in LOAD cases, reflecting the severity of the NFT load as shown at a lower magnification (Fig. 3e–g). Since this ranking order corresponded to the severity of the lesions, aberrant PICALM accumulation in NFTs might indeed be related to the severity of the tauopathy. Strong PICALM immunoreactivity in NFTs and GVD was also found with the HPA019061 antibody (Fig. S2k, n). With the sc-6433 antibody, GVD were weakly stained (Fig. S2l) while NFTs were not (Fig. S2o). The specificity of the labelling with the PICALM antibodies used in this study was controlled by pre-absorption of PICALM antibodies with purified GST-PICALM (Fig. S2p–r). Antibody absorption almost abolished PICALM labelling including NFTs, GVD, dystrophic neurites and endothelial cells.

PICALM and tau co-localisation in AD brains

In order to confirm the co-localisation of PICALM with tau in NFTs, dystrophic neurites and in GVD, double immunofluorescent labelling was carried out using different anti-tau antibodies recognising conformational, phosphorylated and caspase-cleaved tau epitopes. Aberrant accumulation of PICALM was observed in more than 85 % of NFTs immunolabelled with all the anti-tau antibodies used in this study (Alz-50, MC1, TG3, AT8, PHF1 and tau-Asp421) (Fig. 4a–r). Whereas PICALM and tau co-localised in

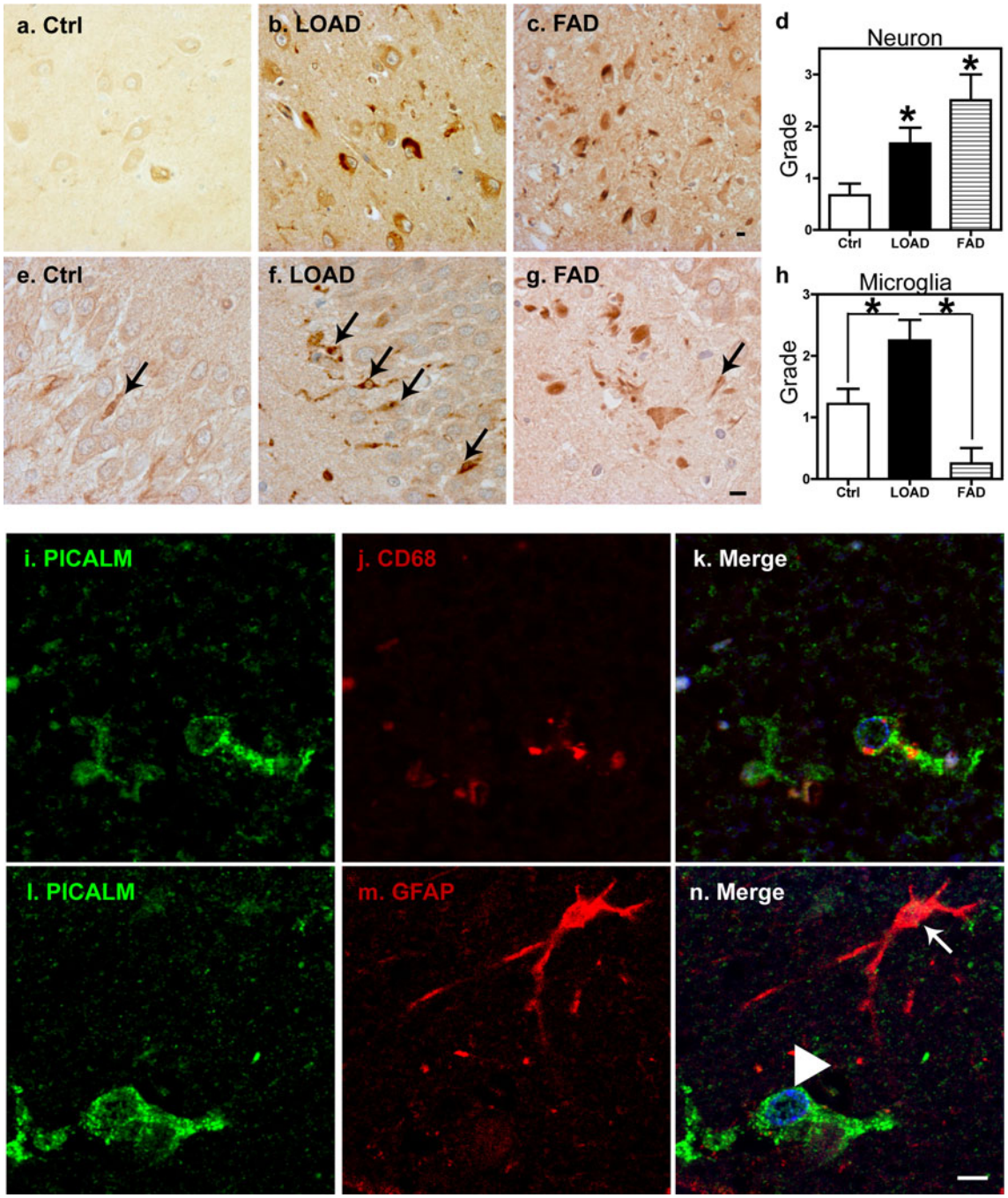

Fig. 2 PICALM immunoreactivity was increased in neurons of AD and microglia of LOAD cases. **a**–**c** PICALM immunoreactivity in neurons of control (**a**), LOAD (**b**) and FAD with PS1 mutation (**c**) cases in the CA4 area of hippocampus. **d** Semi-quantitative estimation of the intensity of PICALM immunoreactivity in PICALM-positive neurons in the hippocampus of control, LOAD and FAD with PS1 mutations. PICALM immunoreactivity was stronger in neuronal cell bodies of AD (**b** and **c**) as compared to control cases (**a**). **e**–**g** PICALM-positive microglial cells (**e**–**g** shown in *black arrows*) were much less frequent in control (**e**) and FAD with PS1 mutations (**g**) than in LOAD brains (**f**). **h** Semi-quantitative estimation of PICALM-positive microglia in the hippocampus of control, LOAD and FAD with PS1 mutations. The intensity of labelling in neurons and the numerical density of microglial cells immunolabelled with PICALM antibody were blindly graded 0–3. (control, $n = 9$; LOAD, $n = 6$; FAD with PS1 mutations, $n = 2$). $^*p < 0.05$, by *ANOVA*. **i**–**k** Hippocampus from a LOAD case was analysed by double immunofluorescent labelling for PICALM (*green*) and CD68 (*red*). PICALM was highly expressed in the activated microglia. **l**–**n** Hippocampus from a LOAD case analysed by double immunofluorescent labelling for PICALM (*green*) and GFAP (*red*), a marker of astrocytes. PICALM was hardly expressed in the astrocytes (*white arrow*). PICALM was expressed in an adjacent neuron (*white arrowhead*). DAPI nuclear counterstaining is shown in *blue* (**k**, **n**). *Scale bar* 20 μm

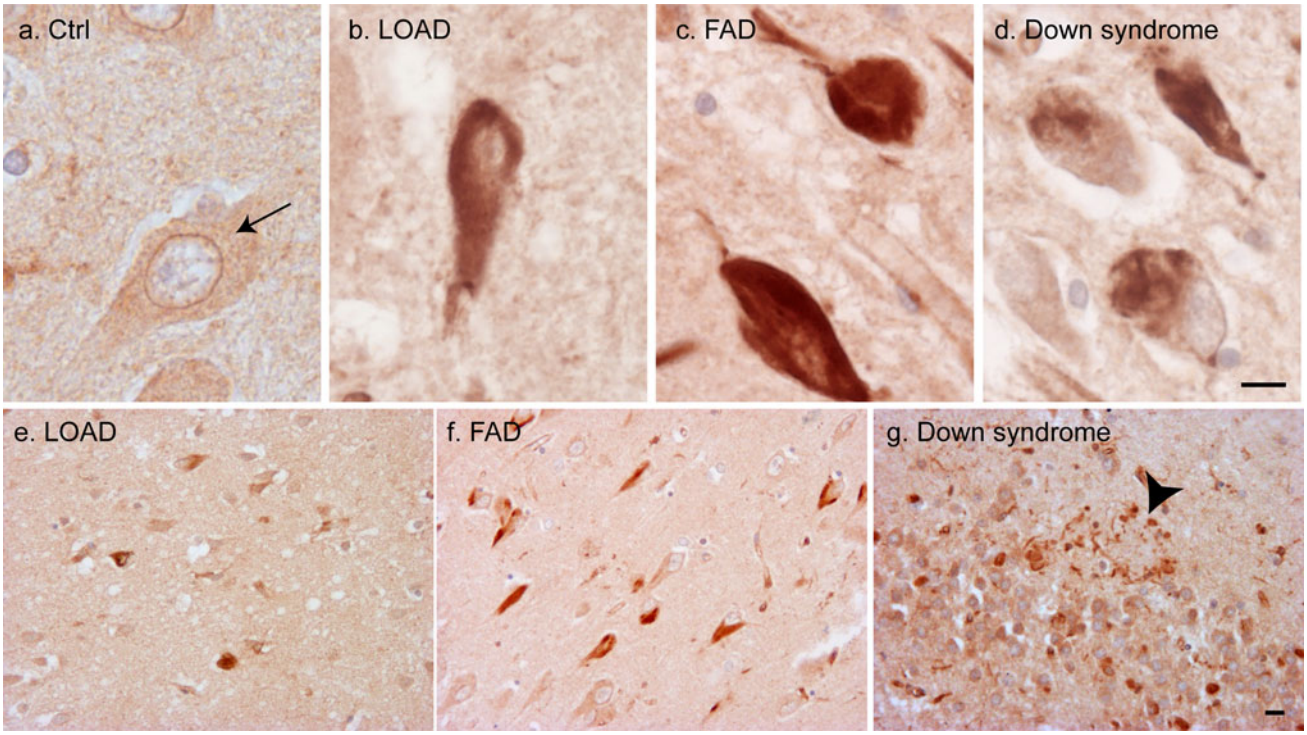

Fig. 3 NFTs in LOAD, FAD and Down syndrome were immunoreactive for PICALM Immunoreactivity of anti-PICALM (HPA019053) antibody in the CA4 region of the hippocampus of a non-demented control case (**a**), or of LOAD (**b**, **e**), FAD (**c**, **f**) and down syndrome (**d**, **g**) patients. The *black small arrow* shows a perinuclear and cytoplasmic PICALM immunoreactivity in a neuron from a control case (**a**). In the LOAD, FAD, and Down syndrome patients, a strong PICALM immunoreactivity was detected in NFT and in GVD. The density of PICALM-positive NFTs correlated with the severity of NFT pathology. Dystrophic neurites associated with amyloid plaques were also PICALM positive (**g** *arrowhead*). *Scale bar* 20 μm

NFTs, PICALM immunoreactivity was often stronger in the core than at the edge of NFTs. PICALM co-localised with tau in dystrophic neurites around the amyloid plaques (Fig. 4d–f) and in GVD (Fig. 4m–o). In AD cases, only few tau-negative neurons were strongly PICALM positive (<5 % of the neuronal population of CA4) (Fig. 4c, white arrowhead). PICALM staining was more diffuse in the cytoplasm of the non-NFT neurons than in NFT. The co-localisation of tau and PICALM was confirmed with anti-PICALM HPA019061 polyclonal antibody, but not with anti-PICALM C-terminal sc-6433 antibody (data not shown).

Co-localisation of PICALM and pTau immunoreactivity was observed in fibrillar NFTs, but neither in pre-tangles nor in extracellular ghost tangles

Granular AT8-positive structures in AD brains are characteristic of pre-tangle neurons [10, 46]. We found that PICALM did not co-localise with pre-tangles bearing AT8-positive punctate structures (Fig. 5a–c, white arrow). To further analyse the association of PICALM with NFT, immunolabelling for PICALM was combined with staining for thiazin red (Fig. 5d–f). Thiazin red is a fluorochrome with a high affinity to fibrillary structures [47, 70]. We found that more than 70 % of thiazin red-stained NFTs were PICALM positive. Extracellular ghost tangles, on the contrary, were not, or only weakly, immunolabelled by the anti-PICALM antibody (Fig. 5d–f, arrowhead).

Immunoelectron microscopy showed that PICALM was associated with PHFs in situ

PICALM labelling of NFTs was confirmed by immunoelectron microscopy (Fig. 5g). Ultrathin sections of post-mortem AD tissues were analysed by immunogold labelling for PICALM (Fig. 5g). PHF structures in NFTs were clearly labelled with the PICALM antibody, although the density of gold particles over the PHFs was moderate. The positive control with PHF1 antibody showed a strong labelling of PHF (Fig. 5h). PHF were not labelled in the negative control in which the primary antibody had been omitted (Fig. 5i).

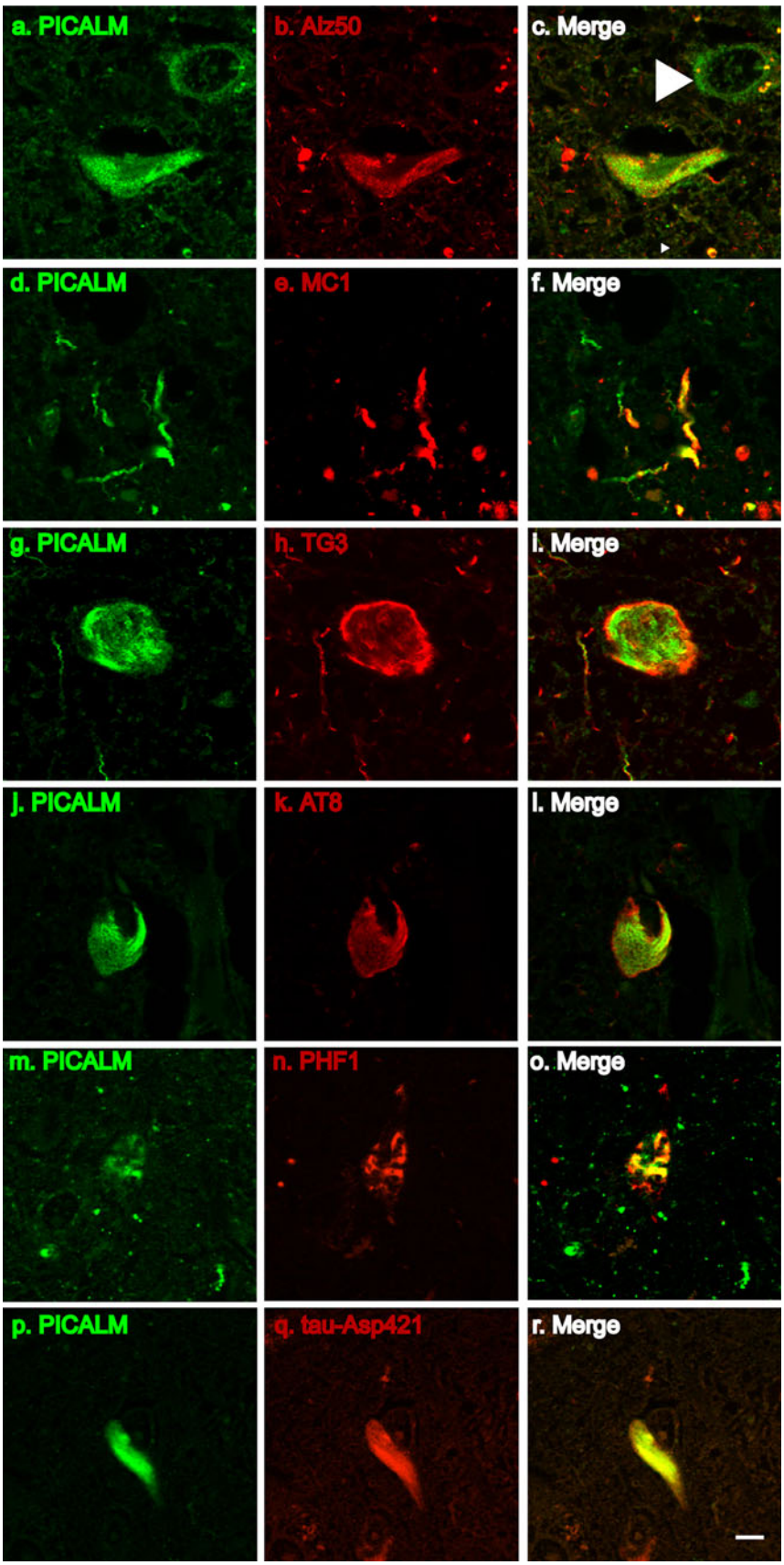

Fig. 4 PICALM and tau co-localisation in NFT in the hippocampus of LOAD. Immunocytochemical co-localisation of PICALM and tau in NFT, using anti-PICALM (HPA019053) and several anti-tau antibodies: Alz50 (**a–c**), MC1 (**d–f**), TG3 (**g–i**), AT8 (**j–l**), PHF1 (**m–o**) and tau-Asp421 (**p–r**). PICALM (*green*) and tau (*red*) were partially or fully co-localised in NFT (**a–c**, **g–l**, **p–r**), in neuropil threads (**d–f**) or in GVD (**m–o**). A few neurons had strong PICALM immunoreactivity devoid of tau immunoreactivity (**c**, *white arrowhead*). *Scale bar* 20 μm

Hyperphosphorylated tau was co-immunoprecipitated with PICALM from AD brain lysate

In order to investigate whether PICALM and hyperphosphorylated tau interacted, proteins were immunoprecipitated from the RIPA-soluble lysate of AD isocortex using anti-PICALM HPA019053 antibody (Fig. 6). PHF1-positive hyperphosphorylated tau was found to be co-immunoprecipitated with PICALM. In the control condition without primary antibody, only trace of non-specific interaction between beads and tau was found (Fig. 6). There was no Aβ immunoreactivity detected in PICALM immunoprecipitates (data not shown).

PHFs purified by sarkosyl fractionation were not immunoreactive

To further analyse the association of PHFs and PICALM in AD brains, a sarkosyl-insoluble fraction enriched in PHFs was prepared [14, 28]. One percent *N*-lauroylsarcosine sodium salt was added to RIPA-soluble brain lysates. The sarkosyl-insoluble pellet, after ultracentrifugation, was enriched in PHFs (composed of PHF-tau proteins). The PHFs present in the sarkosyl-insoluble fraction were analysed by electron microscopy after PICALM immunogold labelling. They were hardly labelled with the anti-PICALM HPA019053 antibody (Fig. S3a, black arrows), and strongly labelled with the PHF1 antibody (Fig. S3b). The specificity of immunogold labelling was verified by a negative control without primary antibody (Fig. S3c). We next analysed PICALM in the sarkosyl-insoluble fraction by western blotting. Hyperphosphorylated tau proteins were enriched in the sarkosyl-insoluble fraction of the AD cases (Fig. S3d), but PICALM immunoreactivity was absent both in AD and control cases (Fig. S3d). These data suggest that PICALM is not an integral component of PHFs.

PICALM was not associated with Aβ in the AD brain

Since PICALM has recently been reported to be involved in APP processing [74], a double immunofluorescence for PICALM and Aβ was carried out in order to examine a potential association between PICALM and amyloid plaques (Fig. 7a–c). PICALM immunoreactivity was found in the dystrophic neurites of the corona, but not in the core, of the amyloid plaques.

PICALM was neither associated with tau in P301L *MAPT* mutation nor with α-synuclein in Lewy body

PICALM immunoreactivity was not co-localised with NFT tau in affected brain areas of a P301L *MAPT* mutation (Fig. 7d–f). In a case of LBD, PICALM immunoreactivity was not found in the α-synuclein-positive Lewy bodies (Fig. 7g–i).

PICALM was cleaved by both calpain and caspase

It was previously reported that recombinant calpain and caspase-3 cleave PICALM in vitro [37, 58]. The increased levels of 50 and 25 kDa PICALM fragments in AD could thus result from proteolytic cleavage by calpain and/or caspase-3. To test the effect of calpain on PICALM, lysates from a control human isocortex and from SY5Y neuroblastoma cells were incubated for 1 h at 22 °C in the presence of $CaCl_2$ to induce calpain digestion. As a result, the longest isoforms of PICALM full-length protein around 65–75 kDa were decreased and the 50 kDa PICALM fragment was increased in the lysates of both human brain and SY5Y neuroblastoma cells (Fig. 8a, b). On the contrary, both calcium chelating agents (EDTA + EGTA) and calpain inhibitors efficiently reduced PICALM cleavage in human brain and SY5Y neuroblastoma cells. The level of the 25 kDa PICALM fragment was not modified in the brain lysate (Fig. 8a), and was not even detected in SY5Y neuroblastoma cells.

To explore the role of caspase in PICALM cleavage, SY5Y neuroblastoma cells were treated with 100 nM staurosporine overnight to activate the apoptotic cascade (Fig. 8c). The level of full-length PICALM isoforms was slightly reduced, with moderate increase in the level of a 50 kDa band. The 25 kDa fragment could not be detected in SY5Y neuroblastoma cells. These data suggest that cleavage of PICALM is both calpain and caspase dependant, and that calpain might be more efficient than caspases in generating the 50 kDa fragment.

Discussion

Two SNPs in the *PICALM* gene have been recently identified as risk factors for LOAD yet the contribution of PICALM to AD pathogenesis is not well understood so far. In the current study, we assessed for the first time in post-mortem AD brains the levels of PICALM. We found that levels of PICALM at 65–75 kDa were significantly decreased, whereas the levels of its cleaved 25 and 50 kDa fragments were significantly increased in AD brains. Both calpain and caspase activation produces a 50 kDa PICALM fragment in vitro. The fragment was, however, much less abundant after caspase activation than after calpain digestion. In addition, we observed PICALM immunoreactivity in most NFTs on the brain slices from the hippocampus and isocortex of LOAD, FAD and Down syndrome brains, but not in NFT of P301L *MAPT* mutation nor in Lewy bodies

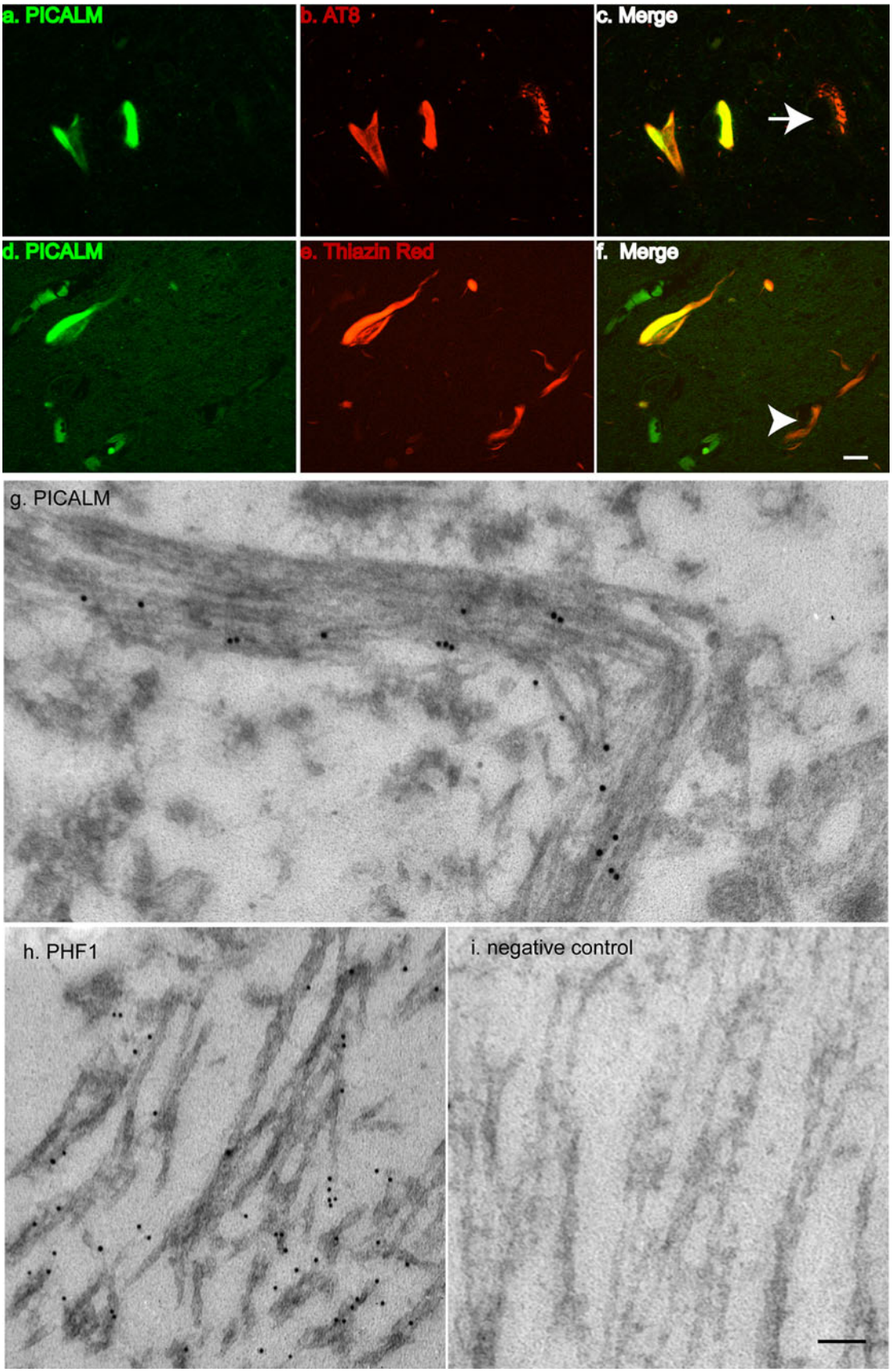
a. PICALM
b. AT8
c. Merge
d. PICALM
e. Thiazin Red
f. Merge
g. PICALM
h. PHF1
i. negative control

◀**Fig. 5** PICALM was associated with PHF-tau, but not with pretangles or extracellular NFTs. **a–c** Double immunofluorescent labelling for PICALM (*green*) and AT8 (*red*). Whereas two mature NFTs are strongly PICALM positive, the pretangle (*white arrow*) showing more diffuse AT8-positive granular deposits was not PICALM positive. **d–f** Fluorescent labelling for PICALM (*green*) combined with staining with thiazin red (*red*). The majority of NFTs stained with thiazin red were PICALM immunoreactive, except for extracellular ghost tangles (*white arrowhead*). *Scale bar* 20 μm. **g** Immunoelectron microscopy of NFTs in a LOAD brain tissue. Abnormal PHF-like filaments present in NFTs were labelled with anti-PICALM HPA019053 antibody (15 nm gold particles). **h** PHF-like filaments were strongly immunolabelled for PHF1 antibody (10 nm gold particles). **i** negative control without primary antibody. *Scale bar* 0.2 μm

of LBD. PICALM-positive microglial cells were also observed to be abundant in AD samples.

PICALM at 65–75 kDa is decreased while 25 and 50 kDa fragments are increased in AD brains

The 75 kDa isoform was particularly lowered. These changes might correspond to variations in translational activity, to post-translational modifications or to an increase in proteolytic cleavage of full-length PICALM. In support of the latter mechanism, we found that levels of 25 and 50 kDa PICALM fragments were increased. The 50 kDa fragment was not labelled by the sc-6433 antibody which recognises the C-terminus (634 a.a. to 651 a.a.) of the full-length protein and was thus probably C-truncated. Enhanced cleavage of PICALM is unlikely due to an increased post-mortem proteolysis since AD and control cases had similar mean post-mortem delays (Table 2). The 65–75 kDa PICALM levels were still decreased after normalisation with the neuronal protein β-tubulin (data not shown), suggesting that decreased PICALM level did not simply result from neuronal loss in AD brain. These results thus provide evidence that PICALM is robustly proteolysed in AD brains.

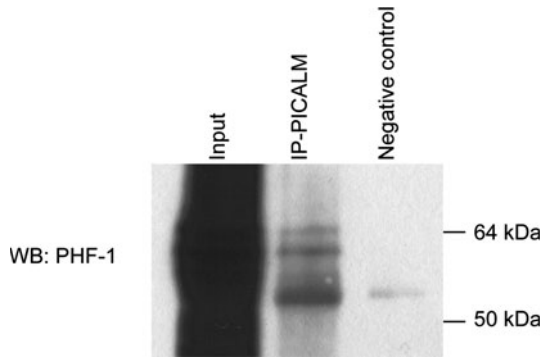

Fig. 6 PICALM was associated with hyperphosphorylated tau. Western blot analysis of PICALM immunoprecipitates from LOAD brain lysate. PHF1-positive hyperphosphorylated tau was co-immunoprecipitated with anti-PICALM HPA019053 antibody. In the control condition where anti-PICALM antibody was absent (negative control), hyperphosphorylated tau was scarcely precipitated with protein G beads

Western blots of PICALM fragments are compatible with cleavage by caspase or calpain

In vitro assays show that PICALM can be cleaved by both calpain and caspase [37, 58]. Calpain is found to be activated in AD brains [59]. Aβ activates, via calcium dysregulation [44], calpain that cleaves a 17-kDa toxic fragment from full-length tau [17, 53]. On the other hand, several caspases are activated by Aβ in AD brains [27, 52, 69] and might thus contribute to PICALM cleavage. Tau is another substrate of caspases [25] and its cleavage by caspase-3 might be an early event during NFT formation [20]. We observed that caspase-3 cleaved tau at Asp421 co-localised with PICALM in NFTs. The longest PICALM isoforms such as isoform 1 (652 a.a.) or 3 (645 a.a.), supposedly corresponding to the 75 kDa bands, contain five consensus DxxD motifs for cleavage by caspase 2, 3 and 6: ^{260}DRGD^{263}, ^{263}DIPD^{266}, ^{392}DLLD^{395}, ^{427}DAVD^{430} and ^{538}DDLD^{541} (numbering according to isoform 1, 652 a.a.) [37], whereas the shortest isoforms lack the ^{427}DAVD^{430} motif. The relative resistance of the 64 kD (i.e. shortest) isoforms could be related to the preferential cleavage at the ^{427}DAVD^{430} motif only present in the longer isoforms. Cleavage at ^{427}DAVD^{430} of PICALM isoform 1 (652 a.a.) and 3 (645 a.a.) is expected to generate a 50 kDa N-terminal and a 25 kDa C-terminal fragments that were indeed found in the brain samples. The complete identification of these fragments awaits analysis by mass spectrometry.

In the current study, in vitro activation of both calpain and caspase led to a decrease of full-length PICALM protein around 65–75 kDa and to an increase of a 50 kDa fragment in lysates from non-demented human brain and SY5Y neuroblastoma cells. The western blot profile of brain homogenates from AD brains is compatible both with calpain and caspase cleavage, though in vitro calpain activation had a more pronounced effect than caspase activation in our experimental conditions, giving rise to a profile that better corresponded to the observation made in post-mortem cerebral cortex.

PICALM is expressed in neurons and endothelial cells and is increased in microglia in AD brains

PICALM immunoreactivity was stronger in a subset of neurons that did not contain NFT, possibly indicating that some neurons accumulated PICALM or its fragments. This aberrant PICALM accumulation might result from, or induce, endocytic dysfunction.

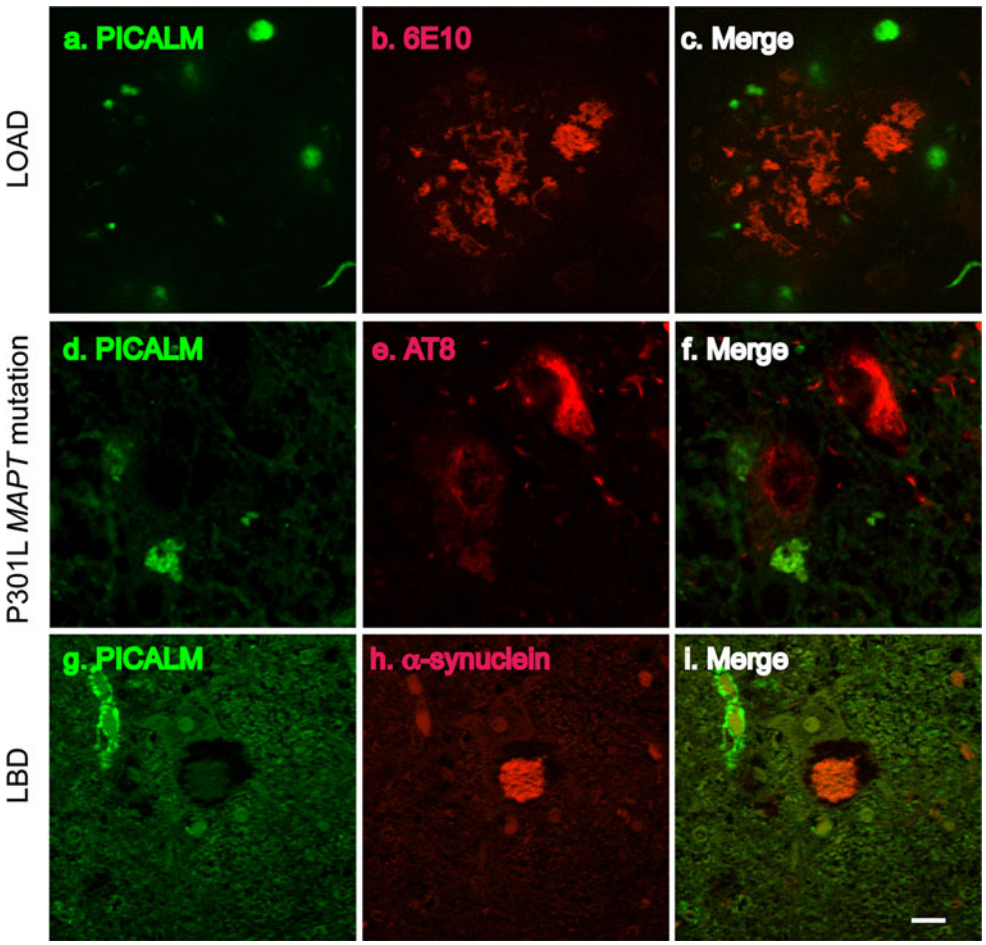

Fig. 7 PICALM was not co-localised with Aβ in AD brains, hyperphosphorylated tau in P301L *MAPT* mutation or α-synuclein in LBD. **a–c** Double immunofluorescent labelling for PICALM (*green*) and 6E10 (*red*) in a LOAD brain tissue. Dystrophic neurites around amyloid plaques were PICALM positive, while amyloid plaques were not. **d–f** Double immunofluorescent labelling for PICALM (*green*) and AT8 (*red*) in the frontal cortex of P301L *MAPT* mutation case. PICALM was not detected in NFT. **g–i** Double immunofluorescent labelling for PICALM (*green*) and α-synuclein (*red*) in the substantia nigra of a LBD case. PICALM was not detected in the Lewy body. *Scale bar* 20 μm

Using the anti-PICALM HPA019053 antibody we observed a strong expression of PICALM in endothelial cells, in ependymocytes and in epithelial cells of the choroid plexus in addition to neurons. This pattern of immunoreactivity was consistent with previous studies using the goat polyclonal anti-PICALM C-terminal antibody (sc-6433) [4]. The aberrant proteolysis of PICALM might affect the function of endothelial cells during the progression of AD, and could be related to dysfunction in the clearance of Aβ peptide.

PICALM was found to be highly expressed in microglia in LOAD brains. It might have been the consequence of microglial activation. Microglial activation plays a role in the clearance of amyloid plaques [60]. While increased Aβ production is the mechanism in probably all FAD cases, decreased amyloid clearance could be involved in LOAD [35]. We found a large difference in the levels of PICALM staining in microglial cells in LOAD and FAD cases, and we speculate that such abnormal accumulation of PICALM in microglial cells might be related to changes in amyloid clearance in LOAD cases. Dysregulated microglial endosomal activity related to increased PICALM cleavage is not excluded but will need additional investigations. Alternatively, activated microglia environment could induce cleavage of PICALM.

PICALM is associated with NFTs in situ in the AD brain

By immunohistochemistry with two independent polyclonal antibodies whose epitopes are located in the middle region of PICALM, we observed immunoreactivity in most NFTs of LOAD, FAD and Down syndrome cases. This observation was confirmed by electron microscopy showing that PHFs were PICALM immunoreactive in ultrathin sections. Since PICALM and tau do not share significant

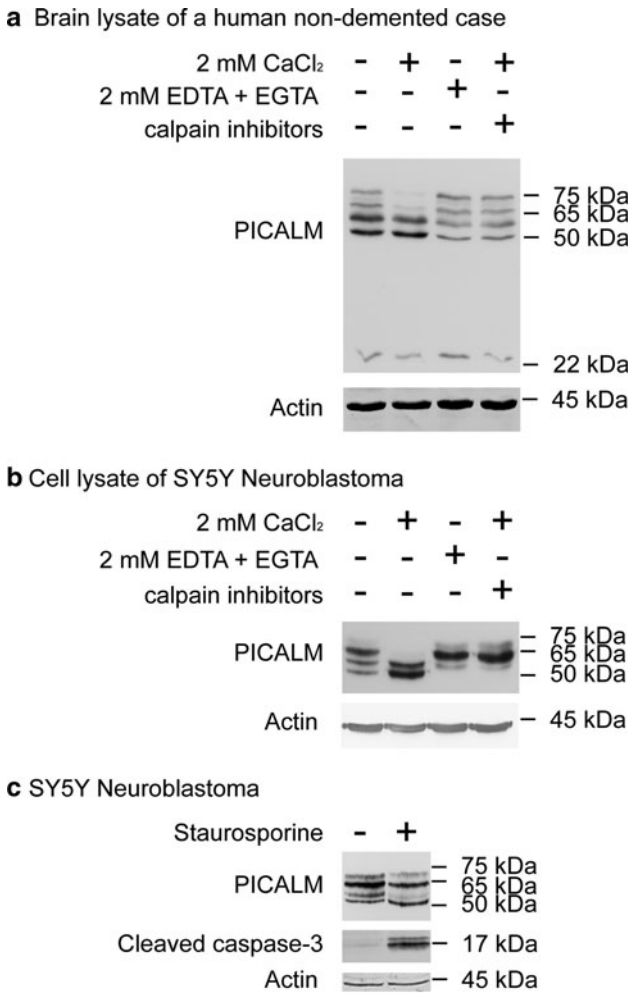

Fig. 8 PICALM was cleaved by calpain and caspase. **a**, **b** Lysates from a human control isocortex (**a**) and SY5Y neuroblastoma cells (**b**) were incubated at 22 °C for 1 h in the presence of 2 mM $CaCl_2$, 2 mM EDTA plus EGTA, or 2 mM $CaCl_2$ plus calpain inhibitors, followed by western blotting for PICALM and actin. **c** SY5Y neuroblastoma cells were treated without or with 100 nM staurosporine for 24 h. Cells were collected and protein extracts were analysed by western blotting for PICALM, cleaved caspase-3 and actin

sequence homologies, it is unlikely that cross-reactivity explains the immunopositivity. NFT labelling with PICALM antibodies was abolished after pre-absorption with PICALM. In addition, PICALM and PHF-tau proteins were co-immunoprecipitated from human AD brain. These observations strongly suggest that PICALM and PHF-tau proteins are associated in NFT. Their interaction was, however, lost during the sarkosyl fractionation. This is not unexpected since several proteins such as the kinases GSK3β or AMPK, interacting with tau during the progression of AD pathology are not enriched in sarkosyl-insoluble fractions [45, 71]. It indicates that PICALM is not an integral constituent of NFTs but interacts with them.

NFTs were not labelled by the anti-PICALM C-terminal antibody sc-6433 as previously reported [4]. These data suggest that PICALM immunoreactivity in NFTs is due to species lacking the C-terminal domain of PICALM, possibly corresponding to the 50 kDa fragment identified by western blotting. This PICALM C-truncated fragment may be large enough to contain the membrane-associating domain localised at the extremity of the N-terminal domain of PICALM [24]. Since binding of tau to membrane phospholipids induces tau aggregation [39], we speculate that cleavage of PICALM might participate in re-localisation of PICALM and tau to membrane structures and promote tau fibrillisation.

Alz50 and MC1-positive neurons as well as NFT were PICALM positive. AT8-positive pre-tangles and ghost tangles were negative. The Alz50 epitope appears after the AT8 epitope in pretangles [46]. Extracellular NFTs have lost some phospho-tau epitopes (such as AT8) and part of the tau sequence [10]. The profile of PICALM immunoreactivity is thus compatible with a time sequence in which PICALM accumulates with phosphorylated and conformationally modified tau in late pretangles, is associated with fibrillar tau in classic fibrillar NFTs and is finally removed from extracellular NFTs.

In addition to NFTs and dystrophic neurites, hyperphosphorylated tau is also detected in GVD [8, 21, 32] and is co-localised with various tau kinases [31, 45, 75]. We showed that PICALM was also co-localised with phospho-tau in GVD. The specificity of GVD labelling was verified with pre-absorption with GST-PICALM.

We wondered if PICALM association was linked to the aggregation state of the protein. This is why we tested another type of NFT, associated with the P301L mutation of *MAPT*. The absence of co-localisation of PICALM with P301L NFTs shows that aggregation alone is not responsible. Similarly, Aβ deposits and Lewy body α-synuclein aggregates were PICALM negative. We are currently testing systematically PICALM immunoreactivity in various tauopathies (work in progress).

PICALM could be involved in endocytic dysfunctions in AD

Given that the cleaved PICALM is unable to promote the assembly of clathrin triskelia into clathrin cage [37], the activity of PICALM must be reduced in AD. Previously, it was reported that knock-down of PICALM causes an enlargement of endosomal compartment and a disruption of TGN/endosomal system in non-neuronal cells [48], or defects in synaptic vesicle size and density as well as a remarkable dendritic retraction in cultured neurons [16, 55]. In addition, acute knock-down of PICALM inhibits endocytosis of VAMP/synaptobrevin [38, 49]. Strikingly,

enlarged endosomes have been observed in the pyramidal hippocampal neurons of LOAD patients [18], where BACE1 co-localisation with phosphorylated APP is increased [43]. Also, dendritic changes in AD are well established [2]. The level of synaptobrevin itself is decreased in AD brains, and its level negatively correlates with cognitive function of AD patients [64]. Altogether, proteolysis of PICALM and reduced level of full-length PICALM that we describe in this study are likely to be associated with synaptic defects and dysfunction of vesicle sorting observed in AD brains [54].

Moreover, PICALM is a partner of AP-2, which initiates clathrin-coated vesicle formation, and AP-2 can also be cleaved by calpain and was observed to be proteolysed in some AD cases [58]. Furthermore, increased calpain activation leads to truncations of dynamin I [36] and amphiphysin I [73]. The degradation/cleavage of several endocytic proteins could thus be an important mechanism leading to endocytic dysfunction in AD [54].

PICALM does not interact with aggregated or oligomeric Aβ

The effects of PICALM on Aβ production remain unclear. In vitro studies have suggested that knocking-down PICALM did not alter the production of toxic Aβ in SY5Y neuroblastoma cells [72] or, on the contrary, reduced both APP internalisation and Aβ production in N2a neuroblastoma cells [74]. PICALM knock-down in APP/PS1 transgenic mice decreased soluble and insoluble Aβ levels and amyloid plaque loads, while overexpression of PICALM increased amyloid pathology [74]. PICALM overexpression, however, appears to protect against Aβ toxicity in yeast, *C. elegans* and cultured rat cortical neurons [68]. The effects of PICALM on production and toxicity of Aβ might thus differ between experimental systems, and the in vivo pathological situation in AD. We could not detect any PICALM immunoreactivity associated to the amyloid deposit in the core of amyloid plaques or Aβ immunoreactivity in PICALM immunoprecipitates from a human LOAD brain lysate. These data suggest that PICALM does not directly interact with aggregated or oligomeric Aβ.

Several independent studies have found 2 SNPs at its 5′ end of *PICALM* gene as being associated with a higher risk for LOAD [29, 34, 41, 42]. It will now be interesting to study how these SNPs affect mRNA/protein expression, alternative splicing and cleavage of PICALM.

In summary, we show for the first time that PICALM is abnormally cleaved and accumulated in tangle containing neurons of AD and Down syndrome brains. Taken together, these data indicate that PICALM, a GWAS-revealed genetic risk factor for AD, is vulnerable to proteolysis and is associated with tau pathology. Inhibition of PICALM proteolysis could have a beneficial effect and appear as a new therapeutic target.

Acknowledgments This study was supported by ANR Franco-Canada CholAD, INSERM (U975-P-A1L4-RP-RPV10014DDA-R10178DD), by MassImage, INSERM (U975-P-A1L4-RP-RPV10015DDA-R10179DD), by grants from dotation d'équipe, INSERM, and by "Investissements d'avenir" ANR-10-IAIHU-06 to C.D., as well as by grants from the Diane programme (Walloon region) (816856), FRMA/SAO, and the Fonds de la Recherche Scientifique Médicale (3.4504.10) to J.P.B. The brain tissues were kindly provided by the GIE NeuroCEB Brain Bank (France Alzheimer, France Parkinson, ARSEP, CSC). We thank Dr Peter Davies for providing anti-tau antibodies, Drs George and Clayton for anti-α synuclein antibody and Dr. Sabrina Turbant for human tissue preparation. Analysis by confocal microscopy was performed at the cellular imaging platform of Pitié-Salpêtrière PICPS.

References

1. Ahle S, Ungewickell E (1986) Purification and properties of a new clathrin assembly protein. EMBO J 5:3143–3149
2. Anderton BH, Callahan L, Coleman P et al (1998) Dendritic changes in Alzheimer's disease and factors that may underlie these changes. Prog Neurobiol 55:595–609
3. Ando K, Leroy K, Heraud C et al (2011) Accelerated human mutant tau aggregation by knocking out murine tau in a transgenic mouse model. Am J Pathol 178:803–816
4. Baig S, Joseph SA, Tayler H et al (2010) Distribution and expression of PICALM in Alzheimer disease. J Neuropathol Exp Neurol 69:1071–1077
5. Ball M, Braak H, Coleman P et al (1997) Consensus recommendations for the postmortem diagnosis of Alzheimer's disease. The National Institute on Aging, and Reagan Institute Working Group on Diagnostic Criteria for the Neuropathological Assessment of Alzheimer's Disease. Neurobiol Aging 18:S1–S2
6. Bertram L, McQueen MB, Mullin K, Blacker D, Tanzi RE (2007) Systematic meta-analyses of Alzheimer disease genetic association studies: the AlzGene database. Nat Genet 39:17–23
7. Boettner DR, Chi RJ, Lemmon SK (2012) Lessons from yeast for clathrin-mediated endocytosis. Nat Cell Biol 14:2–10
8. Bondareff W, Wischik CM, Novak M, Roth M (1991) Sequestration of tau by granulovacuolar degeneration in Alzheimer's disease. Am J Pathol 139:641–647
9. Bossers K, Wirz KT, Meerhoff GF et al (2010) Concerted changes in transcripts in the prefrontal cortex precede neuropathology in Alzheimer's disease. Brain 133:3699–3723
10. Braak E, Braak H, Mandelkow EM (1994) A sequence of cytoskeleton changes related to the formation of neurofibrillary tangles and neuropil threads. Acta Neuropathol 87:554–567
11. Braak H, Braak E (1991) Neuropathological stageing of Alzheimer-related changes. Acta Neuropathol 82:239–259
12. Brion JP, Couck AM, Passareiro E, Flament-Durand J (1985) Neurofibrillary tangles of Alzheimer's disease: an immunohistochemical study. J Submicrosc Cytol 17:89–96
13. Brion JP, Hanger DP, Bruce MT, Couck AM, Flament-Durand J, Anderton BH (1991) Tau in Alzheimer neurofibrillary tangles. N- and C-terminal regions are differentially associated with paired helical filaments and the location of a putative abnormal phosphorylation site. Biochem J 273(Pt 1):127–133
14. Brion JP, Hanger DP, Couck AM, Anderton BH (1991) A68 proteins in Alzheimer's disease are composed of several tau

isoforms in a phosphorylated state which affects their electrophoretic mobilities. Biochem J 279(Pt 3):831–836
15. Brion JP, Power D, Hue D, Couck AM, Anderton BH, Flament-Durand J (1989) Heterogeneity of ubiquitin immunoreactivity in neurofibrillary tangles of Alzheimer's disease. Neurochem Int 14:121–128
16. Bushlin I, Petralia RS, Wu F et al (2008) Clathrin assembly protein AP180 and CALM differentially control axogenesis and dendrite outgrowth in embryonic hippocampal neurons. J Neurosci 28:10257–10271
17. Canu N, Dus L, Barbato C et al (1998) Tau cleavage and dephosphorylation in cerebellar granule neurons undergoing apoptosis. J Neurosci 18:7061–7074
18. Cataldo AM, Peterhoff CM, Troncoso JC, Gomez-Isla T, Hyman BT, Nixon RA (2000) Endocytic pathway abnormalities precede amyloid beta deposition in sporadic Alzheimer's disease and Down syndrome: differential effects of APOE genotype and presenilin mutations. Am J Pathol 157:277–286
19. Coleman PD, Yao PJ (2003) Synaptic slaughter in Alzheimer's disease. Neurobiol Aging 24:1023–1027
20. Cotman CW, Poon WW, Rissman RA, Blurton-Jones M (2005) The role of caspase cleavage of tau in Alzheimer disease neuropathology. J Neuropathol Exp Neurol 64:104–112
21. Dickson DW, Ksiezak-Reding H, Davies P, Yen SH (1987) A monoclonal antibody that recognizes a phosphorylated epitope in Alzheimer neurofibrillary tangles, neurofilaments and tau proteins immunostains granulovacuolar degeneration. Acta Neuropathol 73:254–258
22. Dourlen P, Ando K, Hamdane M, Begard S, Buee L, Galas MC (2007) The peptidyl prolyl cis/trans isomerase Pin1 downregulates the Inhibitor of Apoptosis Protein Survivin. Biochim Biophys Acta 1773:1428–1437
23. Dreyling MH, Martinez-Climent JA, Zheng M, Mao J, Rowley JD, Bohlander SK (1996) The t(10;11)(p13;q14) in the U937 cell line results in the fusion of the AF10 gene and CALM, encoding a new member of the AP-3 clathrin assembly protein family. Proc Natl Acad Sci USA 93:4804–4809
24. Ford MG, Pearse BM, Higgins MK et al (2001) Simultaneous binding of PtdIns(4,5)P2 and clathrin by AP180 in the nucleation of clathrin lattices on membranes. Science 291:1051–1055
25. Gamblin TC, Chen F, Zambrano A et al (2003) Caspase cleavage of tau: linking amyloid and neurofibrillary tangles in Alzheimer's disease. Proc Natl Acad Sci USA 100:10032–10037
26. George JM, Jin H, Woods WS, Clayton DF (1995) Characterization of a novel protein regulated during the critical period for song learning in the zebra finch. Neuron 15:361–372
27. Gervais FG, Xu D, Robertson GS et al (1999) Involvement of caspases in proteolytic cleavage of Alzheimer's amyloid-beta precursor protein and amyloidogenic A beta peptide formation. Cell 97:395–406
28. Greenberg SG, Davies P (1990) A preparation of Alzheimer paired helical filaments that displays distinct tau proteins by polyacrylamide gel electrophoresis. Proc Natl Acad Sci USA 87:5827–5831
29. Harold D, Abraham R, Hollingworth P et al (2009) Genome-wide association study identifies variants at CLU and PICALM associated with Alzheimer's disease. Nat Genet 41:1088–1093
30. Hollingworth P, Harold D, Sims R et al (2011) Common variants at ABCA7, MS4A6A/MS4A4E, EPHA1, CD33 and CD2AP are associated with Alzheimer's disease. Nat Genet 43:429–435
31. Hoozemans JJ, van Haastert ES, Nijholt DA, Rozemuller AJ, Eikelenboom P, Scheper W (2009) The unfolded protein response is activated in pretangle neurons in Alzheimer's disease hippocampus. Am J Pathol 174:1241–1251
32. Joachim CL, Morris JH, Selkoe DJ, Kosik KS (1987) Tau epitopes are incorporated into a range of lesions in Alzheimer's disease. J Neuropathol Exp Neurol 46:611–622
33. Jones L, Harold D, Williams J (2010) Genetic evidence for the involvement of lipid metabolism in Alzheimer's disease. Biochim Biophys Acta 1801:754–761
34. Kamboh MI, Minster RL, Demirci FY et al (2012) Association of CLU and PICALM variants with Alzheimer's disease. Neurobiol Aging 33:518–521
35. Karran E, Mercken M, De Strooper B (2011) The amyloid cascade hypothesis for Alzheimer's disease: an appraisal for the development of therapeutics. Nat Rev Drug Discov 10:698–712
36. Kelly BL, Ferreira A (2006) beta-Amyloid-induced dynamin 1 degradation is mediated by N-methyl-D-aspartate receptors in hippocampal neurons. J Biol Chem 281:28079–28089
37. Kim JA, Kim HL (2001) Cleavage of purified neuronal clathrin assembly protein (CALM) by caspase 3 and calpain. Exp Mol Med 33:245–250
38. Koo SJ, Markovic S, Puchkov D et al (2012) SNARE motif-mediated sorting of synaptobrevin by the endocytic adaptors clathrin assembly lymphoid myeloid leukemia (CALM) and AP180 at synapses. Proc Natl Acad Sci USA 108:13540–13545
39. Kunze G, Barre P, Scheidt HA, Thomas L, Eliezer D, Huster D (2012) Binding of the three-repeat domain of tau to phospholipid membranes induces an aggregated-like state of the protein. Biochim Biophys Acta 1818:2302–2313
40. Lacor PN, Buniel MC, Furlow PW et al (2007) Abeta oligomer-induced aberrations in synapse composition, shape, and density provide a molecular basis for loss of connectivity in Alzheimer's disease. J Neurosci 27:796–807
41. Lambert JC, Heath S, Even G et al (2009) Genome-wide association study identifies variants at CLU and CR1 associated with Alzheimer's disease. Nat Genet 41:1094–1099
42. Lambert JC, Zelenika D, Hiltunen M et al (2011) Evidence of the association of BIN1 and PICALM with the AD risk in contrasting European populations. Neurobiol Aging 32(756):e711–e755
43. Lee MS, Kao SC, Lemere CA et al (2003) APP processing is regulated by cytoplasmic phosphorylation. J Cell Biol 163:83–95
44. Lee MS, Kwon YT, Li M, Peng J, Friedlander RM, Tsai LH (2000) Neurotoxicity induces cleavage of p35 to p25 by calpain. Nature 405:360–364
45. Leroy K, Boutajangout A, Authelet M, Woodgett JR, Anderton BH, Brion JP (2002) The active form of glycogen synthase kinase-3beta is associated with granulovacuolar degeneration in neurons in Alzheimer's disease. Acta Neuropathol 103:91–99
46. Luna-Munoz J, Chavez-Macias L, Garcia-Sierra F, Mena R (2007) Earliest stages of tau conformational changes are related to the appearance of a sequence of specific phospho-dependent tau epitopes in Alzheimer's disease. J Alzheimers Dis 12:365–375
47. Mena R, Edwards P, Perez-Olvera O, Wischik CM (1995) Monitoring pathological assembly of tau and beta-amyloid proteins in Alzheimer's disease. Acta Neuropathol 89:50–56
48. Meyerholz A, Hinrichsen L, Groos S, Esk PC, Brandes G, Ungewickell EJ (2005) Effect of clathrin assembly lymphoid myeloid leukemia protein depletion on clathrin coat formation. Traffic 6:1225–1234
49. Miller SE, Sahlender DA, Graham SC et al (2011) The molecular basis for the endocytosis of small R-SNAREs by the clathrin adaptor CALM. Cell 147:1118–1131
50. Morgan JR, Zhao X, Womack M, Prasad K, Augustine GJ, Lafer EM (1999) A role for the clathrin assembly domain of AP180 in synaptic vesicle endocytosis. J Neurosci 19:10201–10212
51. Naj AC, Jun G, Beecham GW et al (2011) Common variants at MS4A4/MS4A6E, CD2AP, CD33 and EPHA1 are associated with late-onset Alzheimer's disease. Nat Genet 43:436–441
52. Nakagawa T, Zhu H, Morishima N et al (2000) Caspase-12 mediates endoplasmic-reticulum-specific apoptosis and cytotoxicity by amyloid-beta. Nature 403:98–103

53. Nicholson AM, Ferreira A (2009) Increased membrane cholesterol might render mature hippocampal neurons more susceptible to beta-amyloid-induced calpain activation and tau toxicity. J Neurosci 29:4640–4651
54. Nixon RA (2005) Endosome function and dysfunction in Alzheimer's disease and other neurodegenerative diseases. Neurobiol Aging 26:373–382
55. Petralia RS, Wang YX, Indig FE et al (2012) Reduction of AP180 and CALM produces defects in synaptic vesicle size and density. Neuromolecular Med 15:49–60
56. Petralia RS, Yao PJ (2007) AP180 and CALM in the developing hippocampus: expression at the nascent synapse and localization to trafficking organelles. J Comp Neurol 504:314–327
57. Ronca F, Chan SL, Yu VC (1997) 1-(5-Isoquinolinesulfonyl)-2-methylpiperazine induces apoptosis in human neuroblastoma cells, SH-SY5Y, through a p53-dependent pathway. J Biol Chem 272:4252–4260
58. Rudinskiy N, Grishchuk Y, Vaslin A et al (2009) Calpain hydrolysis of alpha- and beta2-adaptins decreases clathrin-dependent endocytosis and may promote neurodegeneration. J Biol Chem 284:12447–12458
59. Saito K, Elce JS, Hamos JE, Nixon RA (1993) Widespread activation of calcium-activated neutral proteinase (calpain) in the brain in Alzheimer disease: a potential molecular basis for neuronal degeneration. Proc Natl Acad Sci USA 90:2628–2632
60. Schenk D, Barbour R, Dunn W et al (1999) Immunization with amyloid-beta attenuates Alzheimer-disease-like pathology in the PDAPP mouse. Nature 400:173–177
61. Seshadri S, Fitzpatrick AL, Ikram MA et al (2010) Genome-wide analysis of genetic loci associated with Alzheimer disease. JAMA 303:1832–1840
62. Sousa R, Tannery NH, Zhou S, Lafer EM (1992) Characterization of a novel synapse-specific protein. I. Developmental expression and cellular localization of the F1–20 protein and mRNA. J Neurosci 12:2130–2143
63. Suzuki M, Tanaka H, Tanimura A et al (2012) The clathrin assembly protein PICALM is required for erythroid maturation and transferrin internalization in mice. PLoS ONE 7:e31854
64. Sze CI, Bi H, Kleinschmidt-DeMasters BK, Filley CM, Martin LJ (2000) Selective regional loss of exocytotic presynaptic vesicle proteins in Alzheimer's disease brains. J Neurol Sci 175:81–90
65. Tebar F, Bohlander SK, Sorkin A (1999) Clathrin assembly lymphoid myeloid leukemia (CALM) protein: localization in endocytic-coated pits, interactions with clathrin, and the impact of overexpression on clathrin-mediated traffic. Mol Biol Cell 10:2687–2702
66. Thal DR, Rub U, Orantes M, Braak H (2002) Phases of A beta-deposition in the human brain and its relevance for the development of AD. Neurology 58:1791–1800
67. Thomas RS, Lelos MJ, Good MA, Kidd EJ (2011) Clathrin-mediated endocytic proteins are upregulated in the cortex of the Tg2576 mouse model of Alzheimer's disease-like amyloid pathology. Biochem Biophys Res Commun 415:656–661
68. Treusch S, Hamamichi S, Goodman JL et al (2011) Functional links between Abeta toxicity, endocytic trafficking, and Alzheimer's disease risk factors in yeast. Science 334:1241–1245
69. Troy CM, Rabacchi SA, Friedman WJ, Frappier TF, Brown K, Shelanski ML (2000) Caspase-2 mediates neuronal cell death induced by beta-amyloid. J Neurosci 20:1386–1392
70. Uchihara T, Nakamura A, Yamazaki M, Mori O (2000) Tau-positive neurons in corticobasal degeneration and Alzheimer's disease–distinction by thiazin red and silver impregnations. Acta Neuropathol 100:385–389
71. Vingtdeux V, Davies P, Dickson DW, Marambaud P (2011) AMPK is abnormally activated in tangle- and pre-tangle-bearing neurons in Alzheimer's disease and other tauopathies. Acta Neuropathol 121:337–349
72. Wu F, Mattson MP, Yao PJ (2010) Neuronal activity and the expression of clathrin-assembly protein AP180. Biochem Biophys Res Commun 402:297–300
73. Wu Y, Liang S, Oda Y et al (2007) Truncations of amphiphysin I by calpain inhibit vesicle endocytosis during neural hyperexcitation. EMBO J 26:2981–2990
74. Xiao Q, Gil SC, Yan P et al (2012) Role of phosphatidylinositol clathrin assembly lymphoid-myeloid leukemia (PICALM) in intracellular amyloid precursor protein (APP) processing and amyloid plaque pathogenesis. J Biol Chem 287:21279–21289
75. Yamazaki Y, Matsubara T, Takahashi T et al (2011) Granulovacuolar degenerations appear in relation to hippocampal phosphorylated tau accumulation in various neurodegenerative disorders. PLoS ONE 6:e26996
76. Yao PJ, Coleman PD, Calkins DJ (2002) High-resolution localization of clathrin assembly protein AP180 in the presynaptic terminals of mammalian neurons. J Comp Neurol 447:152–162
77. Yao PJ, Petralia RS, Bushlin I, Wang Y, Furukawa K (2005) Synaptic distribution of the endocytic accessory proteins AP180 and CALM. J Comp Neurol 481:58–69
78. Yao PJ, Zhu M, Pyun EI et al (2003) Defects in expression of genes related to synaptic vesicle trafficking in frontal cortex of Alzheimer's disease. Neurobiol Dis 12:97–109
79. Ye W, Lafer EM (1995) Clathrin binding and assembly activities of expressed domains of the synapse-specific clathrin assembly protein AP-3. J Biol Chem 270:10933–10939
80. Zhang B, Koh YH, Beckstead RB, Budnik V, Ganetzky B, Bellen HJ (1998) Synaptic vesicle size and number are regulated by a clathrin adaptor protein required for endocytosis. Neuron 21: 1465–1475